

Title:

Evaluation of nanopore sequencing on polar bodies for routine PGT-A

Running title:

Nanopore aneuploidy screening on polar bodies

Authors:

Anna Oberle¹, Franziska Hanzer¹, Felix Kokocinski², Anna Ennemoser¹, Luca Carli¹, Enrico Vaccari¹, Markus Hengstschläger¹, Michael Feichtinger^{1*}

Affiliation:

1 Wunschbaby Institut Feichtinger, Lainzer Straße 6, 1130 Vienna, Austria

2 Gene-Test Bioinformatics Solutions, Jakob-Müller-Str. 16, 68623 Lampertheim, Germany

*Corresponding author: Michael Feichtinger, MD, PhD, EFRM-ESHRE/EBCOG,

michael.feichtinger@wunschbaby.at, +43 1 8777775, Lainzerstrasse 6, 1130 Vienna, Austria

Abstract

STUDY QUESTION:

Is nanopore sequencing for PGT-A analysis of pooled polar bodies a reliable, fast, and cost-effective method and applicable for routine diagnostics in human reproductive care?

SUMMARY ANSWER:

Nanopore sequencing of pooled polar bodies (PB) revealed high concordance rate with traditional array comparative genomic hybridization (aCGH) analysis and the nanopore sequencing workflow was fast (feasible in under 5 hours) and cost-effective (100-150€ per sample), allowing fresh embryo transfer.

WHAT IS KNOWN ALREADY:

PGT-A using PB biopsy derives a clinical benefit by reducing number of embryo transfers and miscarriage rates but is currently not cost-efficient. Results are often unclear and require expert review. Nanopore sequencing technology opens possibilities by providing cost-efficient, fast sequencing results with uncomplicated sample preparation workflows. Interrogating the polar bodies avoids harming the embryo itself and is the only option for PGT-A in some jurisdictions.

STUDY DESIGN, SIZE, DURATION:

In this prospective clinical trial, 102 pooled PB samples from 20 patients treated for infertility between March and December 2022 were analyzed for aneuploidy using nanopore sequencing technology and compared with aCGH results generated as part of the clinical routine. All patients participating in this trial were treated for infertility at 'Wunschbaby Institut Feichtinger' (WIF) in Vienna and chose aneuploidy screening of their polar bodies. All patients provided written informed consent.

PARTICIPANTS/MATERIALS, SETTING, METHODS:

PB samples were analyzed by aCGH for routine PGT-A. Aliquots of whole-genome amplified DNA were anonymized and prepared for sequencing by end-prepping, barcoding and adapter ligation. Samples were pooled equimolar for sequencing on a Nanopore MinION machine. Samples were sequenced for up to 9 hours for 6 pooled PB samples. Whole-chromosome copy-numbers were called by a custom bioinformatic analysis software after alignment and pre-processing. Automatically called results were compared to aCGH results.

MAIN RESULTS AND THE ROLE OF CHANCE:

In total, 99 pooled polar body samples were compared, three samples were excluded because of failed or uninterpretable results. Overall, the Nanopore sequencing workflow showed high concordance rates with aCGH: 96 of 99 samples were consistently detected as euploid or aneuploid (concordance=97%, specificity = 0.957, sensitivity = 1.0, PPV = 0.906, NPV = 1.0) and 91 samples showed a fully concordant karyotype (92%). Chromosomal aneuploidies analyzed in this trial covered all 23 chromosomes with 98 trisomies, 97 monosomies in 70 aCGH samples.

Detailed calculation of time and cost for the nanopore sequencing workflow was performed for different scenarios. Time calculation revealed that the whole nanopore workflow is feasible in under 5 hours (for one sample) with maximum time of 16 hours (for 12 samples in parallel). This enables fresh PB euploid embryo transfer. Material cost for the whole workflow range between 100€ and 150€, including sequencing cost of only 40€ per sample, resulting in cost-efficient aneuploidy screening.

LIMITATIONS, REASONS FOR CAUTION:

For some samples, the reference result remained unclear, due to increased noise and limited resolution of the aCGH method. In particular, the small chromosomes show higher variability in both platforms and manual review is often required. A larger study with follow-up data or a clinical non-selection trial would be beneficial for increased confidence.

WIDER IMPLICATIONS OF THE FINDINGS:

This is the first clinical study, systematically comparing nanopore sequencing for aneuploidy of pooled polar bodies with standard detection methods. High concordance rates confirmed feasibility of nanopore technology for this application. Additionally, the fast and cost-efficient sequencing workflow reveals clinical utility of this technology, making polar body PGT-A clinically attractive.

STUDY FUNDING/COMPETING INTEREST(S):

The study was funded by the Wunschbaby Institut Feichtinger, Dr. Wilfried Feichtinger GmbH. The authors declare no competing conflict of interest.

TRIAL REGISTRATION NUMBER: Not available

Keywords

PGT-A, Polar Body Biopsy, Nanopore Sequencing, Oxford Nanopore Technology, Cost effective PGT-A

1 Introduction

2 With increasing female age, the probability for aneuploid embryos increases and with it the risk of age-
3 related infertility, abortions and children born with trisomy 21 (Franasiak et al., 2014). Early pregnancy
4 loss and spontaneous abortions are most frequently caused by chromosomal abnormalities of the
5 embryo (Petracchi et al., 2009). In contrast to maternal age, paternal age plays a minor role for
6 chromosomal abnormalities (Fonseka and Griffin, 2011). Preimplantation-genetic testing for
7 aneuploidy (PGT-A) is used to screen for unbalanced chromosomal distributions in embryos and can
8 therefore reduce miscarriage rates and improve pregnancy and life-birth rates per embryo-transfer,
9 especially in patients with advanced-maternal age (Feichtinger et al., 2015; Rubio et al., 2017).

10 DNA analyzed in PGT-A can originate from trophoctoderm cells, blastomere cells or polar bodies. All
11 three sources have advantages and specific limitations. While polar body analysis allows the detection
12 of meiotic maternal aneuploidies only, the analysis of trophoctoderm biopsy (TEB) and blastomere
13 biopsy can detect embryogenic aneuploidies. However, blastomere biopsy can possibly damage the
14 embryo (Cohen et al., 2007; Scott et al., 2013) and was shown to provide limited clinical benefit
15 (Mastenbroek et al., 2007). Blastomere biopsy is therefore not commonly performed anymore. In TEB
16 analysis, which is currently seen as the gold standard for PGT-A, diagnosed trophoctoderm
17 aneuploidies might differ from embryogenic material of the inner cell mass due to mosaicisms (Viotti
18 et al., 2021). Embryos classified as aneuploid or mosaic by TEB can lead to euploid, healthy life-births,
19 indicating discordances between inner cell mass and trophoctoderm or self-repair mechanisms (Greco
20 et al., 2015; Treff and Marin, 2021).

21 In contrast, PGT-A using polar body biopsy leaves less room for interpretation, since mitotic errors in
22 cell division leading to mosaicisms are not detected here. In a large multicenter randomized clinical
23 trial ('ESHRE Study into the Evaluation of oocyte Euploidy by Microarray analysis', ESTEEM trial), PGT-
24 A using polar body biopsy was shown to significantly reduce the number of embryo transfer needed
25 for live birth, reduce number of cryopreserved embryos and reduce miscarriage rates (Verpoest et al.,
26 2018). These findings highlight the clinical benefit for PGT-A using polar body biopsy. In contrast to
27 PGT-A using TEB, polar body biopsy allows fresh embryo transfer and can avoid freeze-all procedures.
28 Additionally, due to legal restrictions for TEB analysis in several European countries, polar body biopsy
29 is performed frequently in countries like Germany or Austria (Hengstschlager and Feichtinger, 2005;
30 Ven et al., 2008).

31 However, polar body analysis was stated not to be cost effective using average published costs for
32 PGT-A and IVF/ICSI treatment neither specifically in Germany nor in a universally applicable scenario
33 using data of the ESTEEM trial (Neumann and Griesinger, 2020; Neumann et al., 2020). Average cost
34 per patient (five analyzed oocytes) was stated with around US\$ 5.200 while the threshold for PGT-A to
35 be cost-effective was calculated between US\$ 285 (low-cost scenario) and US\$ 2.204 (high-cost
36 scenario) (Neumann et al., 2020). Therefore, lowering the cost for polar body PGT-A and PGT-A in
37 general is an important goal to improve patient acceptance and to access the clinical benefit for this
38 intervention.

39 PGT-A is often performed using short-read next-generation sequencing (NGS), which requires high
40 initial investment costs and high running expenses. Third-generation sequencing using nanopores is a
41 novel technology with the potential to perform sequencing in a fast, easy, and cost-effective way,
42 enabling application even in small and less well-financed clinics (Cabibbe et al., 2020). Continuous
43 development of the technology led to significant improvements in sequencing quality, accuracy, flow
44 cells and data analysis (Amarasinghe et al., 2020; Jain et al., 2018).

45 Feasibility of long-read nanopore sequencing for PGT was mainly shown for structural variants and
46 monogenetic disease (Cretu Stancu et al., 2017; Hu et al., 2019; Madjunkova et al., 2020; Margolis et

47 al., 2021; Pei et al., 2022), which comes with high costs and is far from clinical routine (Margolis et al.,
48 2021). PGT-A from TEB samples using nanopore sequencing was first demonstrated in a small pilot
49 study, where 9 TEB samples were analyzed with an optimized nanopore protocol and compared to
50 cytogenetic analysis using NGS (Wei et al., 2018). A follow-up study from the same group compared
51 their optimized nanopore aneuploidy analysis of 52 chorionic villi samples, 50 amniotic fluid samples,
52 64 placental or fetal tissue samples and 52 TEB samples with standard NGS PGT-A screening (Wei et
53 al., 2022). Overall, the authors saw very good concordance rates with 100% concordant results for
54 chorionic villi, amniotic fluid and placenta or fetal tissue samples. TEB samples showed one false
55 negative result with a trisomy 21 not being detected by their nanopore sequencing protocol. The
56 optimized nanopore workflow was notably faster (2-6 hours) and more cost-effective (around 50 US\$
57 sequencing cost per sample) compared to traditional NGS screening. Additionally, the workflow was
58 verified by independently trained laboratory technicians with 100% concordance (Wei et al., 2022).
59 This was the first systematic clinical evaluation of nanopore sequencing for aneuploidy including PGT-
60 A with TEB samples. However, due to limited sample number and missing independent external
61 verification of PGT-A samples in this study, further clinical studies are needed to transfer the
62 technology into clinical PGT-A routine analysis.

63 In the present study, pooled polar bodies from 99 oocytes were analyzed using nanopore sequencing
64 and compared to results generated as part of the clinical routine using array comparative genomic
65 hybridization (aCGH). This is the first study that systematically analyses aneuploidy from polar body
66 samples using nanopore sequencing technology including detailed cost analysis of the nanopore
67 sequencing workflow.

68 Material and Methods

69 **Study design and sampling**

70 The present study was designed as a prospective comparative study for aneuploidy analysis of 100
71 pooled polar bodies using the novel nanopore sequencing technology in comparison with standard
72 routine analysis by aCGH. All participating patients were treated for infertility at the 'Wunschbaby
73 Institut Feichtinger' (WIF) in Vienna and chose to perform polar body analysis for aneuploidy of their
74 oocytes. All patients included in this study provided written informed consent. The study was approved
75 by the Ethic Committee of the Medical University Vienna (EK-1249/2022). After oocyte pick-up and
76 fertilization by intracytoplasmic sperm injection (ICSI), both polar bodies were taken simultaneously
77 16 to 18 hours after fertilization and placed in a sterile PCR tube with 2.5 µl of fresh, sterile phosphate-
78 buffered saline (PBS). Opening of the zona pellucida was performed using RI Saturn 5 Active™
79 (Research Instruments Ltd, UK). Polar body samples were frozen at -20°C and transported to an
80 external genetic diagnostic laboratory for routine analysis.

81 **DNA Amplification and reference analysis**

82 PGT-A routine analysis of pooled polar bodies was performed after the standard GentiSure Pre-Screen
83 Kit for Single Cell Analysis Kit (Agilent Technologies, USA) protocol, including Whole Genome
84 Amplification (WGA) with REPLI-g Single Cell Kit using a phi29 polymerase process (QIAGEN, Germany),
85 Fluorescent Labeling and CGH Microarray. This standard protocol was adapted for Polar Body Diagnosis
86 (PBD). Around 5µg of WGA aliquots from pooled polar body samples were anonymized and used for
87 nanopore sequencing.

88 **Nanopore Library Preparation**

89 The library preparation workflow and bioinformatic data analysis pipeline for polar body nanopore
90 sequencing for aneuploidy was set-up and optimized in a pre-clinical study using sequencing of known
91 euploid and aneuploid genomic DNA and single-cells from fibroblast cell lines (Coriell, USA) (Oberle et
92 al., 2022).

93 After receiving anonymized WGA amplified DNA samples, quality was confirmed by 0.8% agarose gel
94 electrophoresis (Thermo Fisher Scientific, USA) and quantity was measured by Qubit 4 fluorometer
95 (Thermo Fisher Scientific, Singapore). Then WGA DNA was purified using gDNA Clean & Concentrator-
96 25 columns (Zymo Research, USA) with elution in 100µl nuclease-free Water (Ambion by Life
97 Technologies, USA).

98 As part of the protocol optimization, around 1.5µg of purified DNA was prepared for some samples by
99 digestion of single-stranded regions using T7 Endonuclease I (New England Biolabs (NEB), UK) to
100 reduce or remove branched structures which were introduced during amplification. DNA was purified
101 using gDNA Clean & Concentrator-25 columns (Zymo Research, USA) and eluted in 50µl nuclease-free
102 water.

103 For library preparation, the Oxford Nanopore Technology (ONT, UK) Kits 'Ligation Sequencing Kit' (SQL-
104 LSK109) and 'Native Barcoding Expansion' (EXP-NBD104) were used according to manufacturer's
105 recommendations.

106 Briefly, for DNA repair and end-preparation, 1-1.5µg purified DNA in 48µl nuclease-free water was
107 added to 2µl NEBNext® FFPE DNA Repair Mix with 3.5µl buffer and 3µl NEBNext® Ultra™ II End-prep
108 Enzyme Mix with 3.5µl buffer (all from NEB, UK) and incubated for 5 minutes at 20°C plus 5 minutes at
109 65°C. The end-prepped DNA was purified using DNA Clean & Concentrator-5 columns (Zymo Research)

110 with elution in 25µl nuclease-free water and purified DNA concentration was measured by Qubit
111 fluorometer.

112 For native barcode ligation, around 500 to 700 ng end-prepped, purified DNA was diluted in 22,5µl
113 nuclease-free water and 2,5µl Native Barcode (ONT) plus 25µl Blunt/TA Ligase Master Mix (NEB) was
114 added, followed by 10 minutes incubation at room temperature. Barcoded DNA was purified using
115 DNA Clean & Concentrator-5 columns (Zymo Research), eluted in 26µl nuclease-free water and
116 concentration was measured using Qubit fluorometer. Purified, barcoded DNA samples for one
117 sequencing run were pooled equimolar in one tube and diluted in 65µl with nuclease-free water.

118 Pooled barcoded samples for one sequencing run (between 4 to 8 samples, see Suppl. Table 1) were
119 ligated to AMII adapters (ONT) by adding 5µl AMII adapter, 20µl NEBNext® Quick Ligation Reaction
120 Buffer and 10µl Quick T4 DNA Ligase (both NEB) and incubated for 10 minutes at room temperature.
121 For the final clean-up, SPRIselect beads (Beckman Coulter, USA) were utilized to ensure elimination of
122 small DNA fragments. 50µl (=0.5x) SPRIselect beads were added to the ligation mix, incubated for 5
123 minutes at room temperature. Beads bound to DNA were pelleted on a magnetic stand, supernatant
124 was removed, and pelleted beads were washed two times with Short Fragments Buffer (SFB, ONT).
125 After the second wash, all remaining SFB was removed, and beads were dried briefly. Dried beads were
126 resuspended thoroughly with 15µl Elution Buffer (ONT) and incubated at room temperature for 10
127 minutes. Beads were pelleted and purified DNA library was transferred into a clean tube and quantified
128 using a Qubit fluorometer.

129 **Nanopore sequencing**

130 The sequencing-ready library was primed and loaded on a MinION R9.4 flow cell (FLO-MIN106D, ONT)
131 according to manufactures recommendation using 25-30 fmol DNA library. Sequencing was performed
132 on MinION Mk1C with simultaneous base calling using standard base calling settings and quality
133 threshold (minimum Q-score) of 8. Sequencing time was adapted according to number of samples
134 pooled and quality of the flow cell (pores available) with average sequencing time of around 9 hours
135 for 6 pooled PB samples resulting in a median number of 105,670 reads (after pre-processing, stdev=
136 76,444) and 210 Mbases (stdev=100) generated per sample (detail sequencing constitution, time and
137 output in Suppl. Table 1).

138 **Data analysis**

139 Nanopore's *MinKNOW* software system controls the raw data acquisition, performing basecalling and
140 demultiplexing with *Guppy* as well as FASTQ file creation. Following on, a data analysis pipeline was
141 applied, developed for long read-based PGT-A data using standard bioinformatics tools and custom
142 software scripts. The specific processing steps are described in the following.

143 Primary data analysis consisted of read cleaning with *Porechop* (Porechop, RRID:SCR_016967) and
144 *Nanofilt* (De Coster et al., 2018), alignment to the human genome GRCh38 with *minimap2* (Li, 2018)
145 and creation of BAM files with *samtools* (Li et al., 2009). Secondary processing steps made use of the
146 *QDNAseq* R software package (Scheinin et al., 2014) and include binning of reads using a custom 500
147 kb bin matrix, GC content and mappability correction, median and reference normalisation,
148 smoothing, segmentation and copy-number calling. A set of five samples were used as a combined
149 reference to capture experiment-specific bias. They represented the first few samples of the study
150 with a representative profile and without whole-chromosome copy-number changes as assessed by
151 aCGH. Further processing was performed to filter and summarize the data, producing a report with
152 genome-wide copy-number plots, noise measurements and automatically detected changes per
153 chromosome and sample.

154 As quality measures of the nanopore sequencing samples, MAPD (Median of the Absolute values of all
155 Pairwise Differences) and noise (median standard deviation of normalised read counts within each
156 segment) values are reported for all chromosomes as well as for each sample and automatically plotted
157 in the chromosomal distribution plots. Samples resulting in a total noise value greater than 0.6 and
158 MAPD value greater than 1.7 were excluded from the comparison (Suppl. Table 1).

159 Results

160 *Study design and nanopore sequencing workflow:*

161 In this study, 102 pooled PB samples from 20 patients were analyzed for PGT-A by nanopore
162 sequencing and compared to clinical routine PGT-A analysis by aCGH. Medium age of all participating
163 patients was 40,5 years (from 35 to 46 years).

164 After PB biopsy 16-18 hours after fertilization, all pooled PB samples were frozen, shipped to the
165 genetic diagnostic laboratory and whole-genome amplification was performed. All samples were
166 successfully amplified while a negative control (culture medium) for each batch showed no
167 amplification and aCGH was performed for all 102 PB samples. WGA aliquots were anonymized and
168 used for nanopore sequencing. Schematic study design is shown in Figure 1.

169 Amplified PB samples were prepared for nanopore sequencing by DNA-repair, end-preparation,
170 Barcode ligation and Adapter ligation. Samples for one nanopore sequencing run were pooled and
171 sequenced on a MinION sequencing machine. For each sequencing run, between four and seven
172 samples were sequenced simultaneously. Flow cells were re-used for maximum of 12 samples. A
173 detailed list showing all sequencing runs and the respective samples is shown in Supplementary Table
174 1. The nanopore sequencing workflow, including data analysis and average time calculation is shown
175 in Figure 2.

176

177 *Detailed time and cost calculation:*

178 To evaluate if nanopore sequencing for PGT-A can be utilized in clinical routine, we performed a
179 detailed time and cost analysis for our nanopore sequencing workflow, which is listed in
180 Supplementary Tables 2 and 3. The nanopore sequencing workflow used in this study starting from
181 amplified DNA until ploidy result is feasible in one and a half hours with one sample being sequenced
182 separately. For 12 samples being sequenced in parallel, we recommend sequencing 6 samples on one
183 flow cell. Then, sample preparation, sequencing and data analysis is feasible in around 12 hours
184 (Supplementary Table 2). Amplification of the pooled polar bodies additionally take between 1.5 hours
185 and 4.5 hours per sample, depending on the kit used for WGA and the number of samples run in
186 parallel. In our study, WGA was performed using REPLig Single Cell Kit (QIAGEN) with a 2.5 h
187 amplification protocol.

188 Material cost for the whole workflow, including WGA, sample preparation, sequencing and data
189 analysis range from 100€ until 220€ per sample. A detailed list of time and cost calculation for different
190 scenarios is shown in Supplementary Table 2 and 3. Initial investment cost for nanopore sequencing
191 can be neglected because prices for nanopore starter packages, where MinION sequencing machines
192 are included cover material costs.

193

194 *Quality control and genome coverage for nanopore sequencing workflow:*

195 In total three samples were excluded from the comparison due to failed or uninterpretable results.
196 Two samples (PB61, PB95) were excluded due to failed or uninterpretable aCGH (2 %) and one sample
197 (PB48) was excluded due to failed quality check after nanopore sequencing with noise and MAPD
198 values below quality threshold (1%).

199 Data analysis from nanopore sequencing results revealed medium sequencing output of 210 Mbases
200 and a median of 105,670 reads per sample (after pre-processing, 70 to 650 Mbases and 32,924 to

201 374,841 reads). A median of 3% (88 Mbases) of the genome was covered by one or more reads
202 (between 0.9 – 9.3%). With the 0.5 Mbases bin matrix applied in the analysis, a smoothing window of
203 6 bins and a calling limit of 20 bins, the application has a theoretical resolution of around 10 Mbases.
204 This is comparable with the common resolution for PGT-A using aCGH or NGS (6-10 Mbases) (Snider
205 et al., 2021). Average Q-score of all nanopore-sequenced samples was 8. Quality was additionally
206 verified in the bioinformatic data analysis pipeline by noise and MAPD values. Average noise of all
207 samples was 0.428 (between 0.230 and 0.724) and average MAPD was 1.164 (between 0.720 and
208 1.809). All noise and MAPD values are listed in Supplementary Table 1 and relationship between both
209 quality measures is visualized in Supplementary Figure 1.

210

211 *Comparison of PGT-A results from nanopore sequencing with routine aCGH results:*

212 In total, 99 pooled PB samples for PGT-A screening were utilized in this study for comparison of ploidy
213 status by routine aCGH and by nanopore sequencing workflow. From these 99 samples, 29 were
214 detected euploid (29.3 %) and 70 were detected aneuploid (70.7 %) by aCGH reference. This is
215 expected, given the patient cohort with medium female age of 40.5 years. Nanopore sequencing
216 analysis detected 32 samples as euploid and 67 as aneuploid resulting in 97% concordance with aCGH
217 analysis and a sensitivity of 0.95, specificity of 1.0 with a positive predictive value (PPV) of 1.0 and a
218 negative predictive value (NPV) of 0.90 (Figure 1). Three samples detected as aneuploid using aCGH
219 revealed an euploid chromosomal pattern using nanopore sequencing. All three samples showed a
220 single aneuploid chromosome (+22, +19, -16, respectively) by aCGH and these elevations or reductions
221 were visible but below threshold at nanopore sequencing, as listed in Supplementary Table 1.

222 In total, aCGH analysis detected 195 aneuploid chromosomes in the 99 samples, with 98 trisomies and
223 97 monosomies covering all 23 chromosomes, shown in Figure 3. Counting the exact match (all
224 chromosomes concordant but assigning “multiple” to karyotypes with more than three aberrations) of
225 nanopore sequencing results with aCGH results, we found 91.9% concordance (91 of 99 samples
226 showing exact match). Segmental changes were not addressed in this study. For all samples, where
227 Endonuclease digest was performed following WGA, the results with Endonuclease digestion were
228 utilized for this comparison (see below). Example chromosomal distribution plots of euploid and
229 aneuploid detected samples, which are automatically created from bioinformatic data analysis pipeline
230 after nanopore sequencing are shown in Figure 4.

231 To assist the physicians and patients in the process of decision-making, a further critical evaluation of
232 euploid-detected PBs can be performed and marginal/borderline elevated or reduced chromosomes
233 can be mentioned together with the euploid result in the clinical report. Here, we performed manual
234 revision of all euploid-detected samples after nanopore sequencing and the additional information
235 about slightly elevated or reduced chromosomes can be found in Supplementary Table 1.

236

237 *Endonuclease digestion step:*

238 As part of this study, we evaluated the importance of an endonuclease digestion step. 28 samples were
239 run in parallel with and without endonuclease digestion step. While samples with a high signal to noise
240 ratio (between copy-number changes and the normal level) show matching results, the additional
241 digestion clearly reduces noise and improves calling for challenging cases. Reduction of average noise
242 and MAPD values, as well as improvements of sequencing-output per time is shown in Figure 5.
243 Detailed comparison of sequencing results with and without endonuclease digest is listed in
244 Supplementary Table 4. For the calculation of concordance between aCGH and nanopore sequencing,

245 results after Endonuclease digest were utilized for all these samples. For all new investigations we
246 recommend adding this step.

247 Discussion

248 The present study is the first study that systematically compares polar body PGT-A analysis using
249 nanopore sequencing with routine aCGH analysis. PGT-A results on pooled polar bodies using novel
250 nanopore sequencing analyses showed high concordance rates compared with routinely performed
251 aCGH.

252 Even though PGT-A through trophectoderm biopsy can be regarded the gold standard of
253 preimplantation genetic testing nowadays, polar body analysis has several advantages.

254 More and more patients undergoing assisted reproduction in Europe and the US are of advanced
255 reproductive age and thus potentially benefitting from PGT-A (European IVF-monitoring Consortium
256 (EIM) et al., 2017). However, those patients tend to have low to very low ovarian reserve leading to
257 poor response to ovarian stimulation. Thus, those treatments often do not result in good quality
258 blastocysts eligible for trophectoderm biopsy and cryopreservation. Furthermore, freeze-all strategies
259 in normal and poor-responders have been shown to reduce cumulative ongoing pregnancy rates
260 compared with fresh embryo transfers (Wong et al., 2021).

261 Polar body analysis allows fresh embryo transfer and reduces unnecessary lab procedures like
262 extended blastocyst culture and cryopreservation of potentially aneuploid embryos. Since the polar
263 bodies represent a byproduct of the oocyte, no essential structure of the future embryo is harmed.
264 Even though polar body analysis covers only the maternal part of meiotic aneuploidies, those are
265 thought to contribute to up to 99% of meiotic aneuploidies with only 1% paternal meiotic aneuploidies
266 (Lodge and Herbert, 2020). Postzygotic mitotic aneuploidies on the other hand might result in mosaic
267 embryos (Treff and Marin, 2021). Mosaic embryos have been shown to have the potential to result in
268 healthy live births, questioning the sensitivity of trophectoderm biopsy and potentially leading to the
269 discardment of healthy embryos diagnosed as aneuploid (Greco et al., 2015; Victor et al., 2019). Polar
270 body analysis on the other hand is not challenged by mosaicism and therefore does not imply this risk.

271 Apart from medical considerations, polar body diagnosis might be applied in countries with legal
272 restrictions to trophectoderm biopsy or embryo cryopreservation.

273 Polar body biopsy compared to untested embryo transfer has been shown to reduce miscarriage rates
274 and to increase pregnancy and live birth rates per euploid transfer in patients of advanced maternal
275 age (Feichtinger et al., 2015; Verpoest et al., 2018). However, up to very recently, polar body biopsy
276 did not prove cost-efficient, resulting in significantly higher costs per patient and per live birth
277 (Neumann et al., 2020).

278 The present study systematically compares PB PGT-A analysis using nanopore sequencing with routine
279 aCGH analysis. The concordance rate between both technologies found in this study was 97% for
280 euploid/aneuploid decision and 92% for exact match. These concordance rates are high, given the
281 different nature of the methods and the delicate sample type of PB biopsy. Similar studies comparing
282 different technologies for PGT-A analysis received slightly higher concordance rates (Kung et al., 2015;
283 Sachdeva et al., 2017; Walters-Sen et al., 2021; Wei et al., 2022). However, genetic material utilized in
284 these studies was originated from trophectoderm biopsy, which comprises significantly more genetic
285 starting material than PB biopsy, resulting in more stable and uniform whole genome amplification.
286 From 102 PB samples analyzed with nanopore sequencing in our study, 101 samples passed the quality
287 threshold, indicating a high reliability of the technology.

288 In a comparable study using nanopore sequencing in comparison with standard clinical detection
289 methods (NGS, FISH, aCGH), discordant aneuploidy results were re-examined and the initial nanopore
290 sequencing results were confirmed in these samples, showing that even established clinical testing

291 methods like FISH or aCGH might result in misdiagnosis (Wei et al., 2022). Misdiagnosis of routine aCGH
292 PGT-A analysis has also been shown previously in a study comparing aCGH with NGS results (Sachdeva
293 et al., 2017). In the present study using material from pooled polar bodies, re-examination of aCGH
294 was not possible due to limited sample resource.

295 Independent of the technology, the analysis of chromosomal material is complicated by the different
296 characteristics of human chromosomes (Piovesan et al., 2019). The short chromosomes 19, 20, 21, 22
297 and Y provide limited material which leads to an increased variability in measurements. The GC-richest
298 chromosomes 16, 17, 19 and 22 often display increased levels of noise. Also chromosomes with
299 heterochromatic polymorphisms, like chromosomes 1, 9 and 16 differ due to normal, benign
300 variations in heterochromatin-content, which can be visualized by microscopy but is hard to interpret
301 in sequencing-based methods or aCGH (Hernandez-Nieto et al., 2021). In our study, the chromosomes
302 9, 19, 21 and 22 showed most discordances (Figure 3).

303 Nanopore sequencing has several advantages, compared to aCGH or NGS analysis, including but not
304 limited to the fast turnaround time, inexpensive sequencing, as well as small initial investment costs
305 needed. These advantages might lead to cost-efficient diagnostics for clinical applications. Time and
306 cost of nanopore sequencing for clinical reproductive healthcare has been reported in several
307 publications, but detailed statements on how these number can be achieved are often not stated
308 (Bartalucci et al., 2019; Cretu Stancu et al., 2017; Wei et al., 2018, 2022). Here, we provide detailed
309 insight in material costs and preparation, sequencing, and data analysis time for different scenarios
310 (Supplementary Table 2 and 3).

311 Several factors significantly influence the laboratory and sequencing time as well as material costs. The
312 main factor influencing the time per sample is the number of samples, that are prepared and
313 sequenced in parallel, mostly influencing sequencing time, but also sample preparation time. The main
314 factor influencing cost per sample is the sample throughput per year, because flow cell price changes
315 significantly with the number of flow cells purchased per year (between 450€ and 900€ per flow cell).
316 Here, we calculate with 48 flow cells per year (approximately 500 samples/year), leading to a flow cell
317 price of 475€ (ONT Store EU, visited in April 2023). Since flow cells can be re-used after sequencing,
318 sequencing price per sample does not change much with lower samples being sequenced in parallel.
319 For one sample, the whole analysis workflow, including WGA, library preparation, sequencing and data
320 analysis is possible in under 5 hours and for 12 samples being prepared in parallel, this workflow is
321 feasible in 14 to 16 hours (Supplementary Table 3), leading to same-day results.

322 The fact that nanopore sequencing, in contrast to aCGH or NGS applications, does not require high
323 initial investment costs, opens the possibility for decentralized diagnostic laboratories associated to
324 IVF clinics. With more, decentralized diagnostic laboratories, transportation of genetic material to
325 large, centralized laboratories is not necessary, again leading to faster turnaround-time. The fast
326 turnaround-time of the optimized nanopore sequencing workflow used in this study opens the
327 possibility for same-cycle transfer of euploid embryos, leading again to a cost reduction by reducing
328 freeze-all procedures and hormonal treatment for the embryo transfer, possibly leading to a shorter
329 time-to-pregnancy.

330 Another advantage of nanopore sequencing compared to aCGH or NGS is the high flexibility of the
331 sequencing method. Sequencing data as well as quality measures of the data generated, and the flow
332 cell health can be monitored in real-time during nanopore sequencing. If more data is required or
333 quality of the library is poor, sequencing can easily be prolonged or repeated on the same flow cell
334 until sufficient amount of data is generated. This can reduce the necessity to repeat uninterpretable
335 results and can reduce prolonged time-to diagnosis.

336 In our study, the data analysis pipeline automatically generates the sequencing plot with significantly
337 abnormal chromosomes being highlighted and quality measures (noise and MAPD) are plotted for each
338 chromosome. Example plots are shown in Figure 4. The karyotype is reported automatically according
339 to the optimized bioinformatic pipeline. This automation together with the clear and easy-to-read
340 karyotype plot makes the nanopore sequencing data very easy to read and understand. Interpretation
341 of the results does not require years of expert knowledge and experience, which is often required for
342 the interpretation of aCGH plots. The automated analysis pipeline is not dependent on subjective
343 decision-making of the responsible geneticist or physician.

344 Nevertheless, following the clinical practice, we additionally performed manual review of all euploid-
345 detected samples (Supplementary Table 1). This additional annotation about small chromosomal
346 aberrations does not change the automatically reported result (euploid) but can be provided as
347 additional information in the medical report. This report can facilitate the embryo prioritization and
348 decision-making for the physician and the patients as part of their fertility treatment.

349 Taken together, pooled polar body nanopore sequencing revealed high concordance rates compared
350 to conventional aCGH with minimized time and financial resources required.

Author's roles

AO, MF, and MH designed the study. AO optimized the nanopore sequencing workflow and supervised the experiments. FH performed the nanopore sequencing, FK performed data analysis. AO, FH, FK, MF, and MH interpreted the results. AO, FH, FK, and MF designed and wrote the manuscript. AE, LC, EV performed PB biopsies and provided insights in embryology. All authors approved the final version of the manuscript.

Acknowledgements

We would like to thank all patients participating in this study! We also thank all staff members from HLN Genetic GmbH for providing the reference samples and for the collaboration in this study.

Funding

The study was funded by the Wunschbaby Institut Feichtinger, Dr. Wilfried Feichtinger GmbH. No external funding was applied for this study.

Conflict of Interest

The authors declare no conflict of interest.

References

- Amarasinghe, S.L., Su, S., Dong, X., Zappia, L., Ritchie, M.E., and Gouil, Q. (2020). Opportunities and challenges in long-read sequencing data analysis. *Genome Biol.* 21.
- Bartalucci, N., Romagnoli, S., Contini, E., Marseglia, G., Magi, A., Guglielmelli, P., Pelo, E., and Vannucchi, A.M. (2019). Long Reads, Short Time: Feasibility of Prenatal Sample Karyotyping by Nanopore Genome Sequencing. *Clin. Chem.* 65, 1604–1605.
- Cabibbe, A.M., Spitaleri, A., Battaglia, S., Colman, R.E., Suresh, A., Uplekar, S., Rodwell, T.C., and Cirillo, D.M. (2020). Application of Targeted Next-Generation Sequencing Assay on a Portable Sequencing Platform for Culture-Free Detection of Drug-Resistant Tuberculosis from Clinical Samples. *J. Clin. Microbiol.* 58.
- Cohen, J., Wells, D., and Munné, S. (2007). Removal of 2 cells from cleavage stage embryos is likely to reduce the efficacy of chromosomal tests that are used to enhance implantation rates. *Fertil. Steril.* 87, 496–503.
- De Coster, W., D’Hert, S., Schultz, D.T., Cruts, M., and Van Broeckhoven, C. (2018). NanoPack: visualizing and processing long-read sequencing data. *Bioinformatics* 34, 2666–2669.
- Cretu Stancu, M., van Roosmalen, M.J., Renkens, I., Nieboer, M.M., Middelkamp, S., de Ligt, J., Pregno, G., Giachino, D., Mandrile, G., Espejo Valle-Inclan, J., et al. (2017). Mapping and phasing of structural variation in patient genomes using nanopore sequencing. *Nat. Commun.* 8, 1326.
- European IVF-monitoring Consortium (EIM), European Society of Human Reproduction and Embryology (ESHRE), Calhaz-Jorge, C., De Geyter, C., Kupka, M.S., de Mouzon, J., Erb, K., Mocanu, E., Motrenko, T., Scaravelli, G., et al. (2017). Assisted reproductive technology in Europe, 2013: results generated from European registers by ESHRE. *Hum. Reprod.* 32, 1957–1973.
- Feichtinger, M., Stopp, T., Göbl, C., Feichtinger, E., Vaccari, E., Mädler, U., Laccone, F., Stroh-Weigert, M., Hengstschläger, M., Feichtinger, W., et al. (2015). Increasing Live Birth Rate by Preimplantation Genetic Screening of Pooled Polar Bodies Using Array Comparative Genomic Hybridization. *PLoS One* 10, e0128317.
- Fonseka, K.G.L., and Griffin, D.K. (2011). Is there a paternal age effect for aneuploidy? *Cytogenet. Genome Res.* 133, 280–291.
- Franasiak, J.M., Forman, E.J., Hong, K.H., Werner, M.D., Upham, K.M., Treff, N.R., and Scott, R.T. (2014). The nature of aneuploidy with increasing age of the female partner: a review of 15,169 consecutive trophectoderm biopsies evaluated with comprehensive chromosomal screening. *Fertil. Steril.* 101.
- Greco, E., Minasi, M.G., and Fiorentino, F. (2015). Healthy Babies after Intrauterine Transfer of Mosaic Aneuploid Blastocysts. *N. Engl. J. Med.* 373, 2089–2090.
- Hengstschläger, M., and Feichtinger, W. (2005). Die erste Präimplantationsdiagnostik in Österreich. *Wien. Klin. Wochenschr.* 117, 725–727.
- Hernandez-Nieto, C., Gayete-Lafuente, S., Alkon-Meadows, T., Lee, J., Luna-Rojas, M., Mukherjee, T., Copperman, A.B., and Sandler, B. (2021). Parental chromosomal heteromorphisms are not associated with an increased risk of embryo aneuploidy. *JBRA Assist. Reprod.* 25, 575–580.
- Hu, L., Liang, F., Cheng, D., Zhang, Z., Yu, G., Zha, J., Wang, Y., Xia, Q., Yuan, D., Tan, Y., et al. (2019). Location of Balanced Chromosome-Translocation Breakpoints by Long-Read Sequencing on the Oxford Nanopore Platform. *Front. Genet.* 10, 1313.
- Jain, M., Koren, S., Miga, K.H., Quick, J., Rand, A.C., Sasani, T.A., Tyson, J.R., Beggs, A.D., Dilthey, A.T., Fiddes, I.T., et al. (2018). Nanopore sequencing and assembly of a human genome with ultra-long

reads. *Nat. Biotechnol.* 2018 364 36, 338–345.

Kung, A., Munné, S., Bankowski, B., Coates, A., and Wells, D. (2015). Validation of next-generation sequencing for comprehensive chromosome screening of embryos. *Reprod. Biomed. Online* 31, 760–769.

Li, H. (2018). Minimap2: pairwise alignment for nucleotide sequences. *Bioinformatics* 34, 3094–3100.

Li, H., Handsaker, B., Wysoker, A., Fennell, T., Ruan, J., Homer, N., Marth, G., Abecasis, G., Durbin, R., and 1000 Genome Project Data Processing Subgroup (2009). The Sequence Alignment/Map format and SAMtools. *Bioinformatics* 25, 2078–2079.

Lodge, C., and Herbert, M. (2020). Oocyte aneuploidy—more tools to tackle an old problem. *Proc. Natl. Acad. Sci. U. S. A.* 117, 11850–11852.

Madjunkova, S., Sundaravadanam, Y., Antes, R., Abramov, R., Chen, S., Yin, Y., Zuzarte, P.C., Moskovtsev, S.I., Jorgensen, L.G.T., Baratz, A., et al. (2020). Detection of Structural Rearrangements in Embryos. *N. Engl. J. Med.* 382, 2472–2474.

Margolis, C., Werner, M., and Jalas, C. (2021). Variant haplophasing by long-read sequencing: proof of concept in preimplantation genetic workup and an opportunity to distinguish balanced and normal embryos. *Fertil. Steril.* 116, 668–669.

Mastenbroek, S., Twisk, M., van Echten-Arends, J., Sikkema-Raddatz, B., Korevaar, J.C., Verhoeve, H.R., Vogel, N.E.A., Arts, E.G.J.M., de Vries, J.W.A., Bossuyt, P.M., et al. (2007). In Vitro Fertilization with Preimplantation Genetic Screening. *N. Engl. J. Med.* 357, 9–17.

Neumann, K., and Griesinger, G. (2020). An Economic Analysis of Aneuploidy Screening of Oocytes in Assisted Reproduction in Germany. *Geburtshilfe Frauenheilkd.* 80, 172–178.

Neumann, K., Sermon, K., Bossuyt, P., Goossens, V., Geraedts, J., Traeger-Synodinos, J., Parriego, M., Schmutzler, A., van der Ven, K., Rudolph-Rothfeld, W., et al. (2020). An economic analysis of preimplantation genetic testing for aneuploidy by polar body biopsy in advanced maternal age. *BJOG An Int. J. Obstet. Gynaecol.* 127, 710–718.

Oberle, A., Carli, L., Ennemoser, A., Hengstschläger, M., and Feichtinger, M. (2022). P-533 Single-cell long-read nanopore sequencing as a fast and cost-efficient method for aneuploidy detection and potentially PGT-A, a pre-clinical study. *Hum. Reprod.* 37.

Pei, Z., Deng, K., Lei, C., Du, D., Yu, G., Sun, X., Xu, C., and Zhang, S. (2022). Identifying Balanced Chromosomal Translocations in Human Embryos by Oxford Nanopore Sequencing and Breakpoints Region Analysis. *Front. Genet.* 0, 2723.

Petracchi, F., Colaci, D.S., Igarzabal, L., and Gadow, E. (2009). Cytogenetic analysis of first trimester pregnancy loss. *Int. J. Gynaecol. Obstet.* 104, 243–244.

Piovesan, A., Pelleri, M.C., Antonaros, F., Strippoli, P., Caracausi, M., and Vitale, L. (2019). On the length, weight and GC content of the human genome. *BMC Res. Notes* 12, 106.

Rubio, C., Bellver, J., Rodrigo, L., Castellón, G., Guillén, A., Vidal, C., Giles, J., Ferrando, M., Cabanillas, S., Remohí, J., et al. (2017). In vitro fertilization with preimplantation genetic diagnosis for aneuploidies in advanced maternal age: a randomized, controlled study. *Fertil. Steril.* 107, 1122–1129.

Sachdeva, K., Discutido, R., Albus, F., Almekosh, R., and Peramo, B. (2017). Validation of Next-Generation Sequencer for 24-Chromosome Aneuploidy Screening in Human Embryos. *Genet. Test. Mol. Biomarkers* 21, 674–680.

Scheinin, I., Sie, D., Bengtsson, H., van de Wiel, M.A., Olshen, A.B., van Thuijl, H.F., van Essen, H.F.,

Eijk, P.P., Rustenburg, F., Meijer, G.A., et al. (2014). DNA copy number analysis of fresh and formalin-fixed specimens by shallow whole-genome sequencing with identification and exclusion of problematic regions in the genome assembly. *Genome Res.* *24*, 2022–2032.

Scott, R.T., Upham, K.M., Forman, E.J., Zhao, T., and Treff, N.R. (2013). Cleavage-stage biopsy significantly impairs human embryonic implantation potential while blastocyst biopsy does not: a randomized and paired clinical trial. *Fertil. Steril.* *100*, 624–630.

Snider, A.C., Darvin, T., Spor, L., Akinwale, A., Cinnioglu, C., and Kayali, R. (2021). Criteria to evaluate patterns of segmental and complete aneuploidies in preimplantation genetic testing for aneuploidy results suggestive of an inherited balanced translocation or inversion. *F&S Reports* *2*, 72–79.

Treff, N.R., and Marin, D. (2021). The “mosaic” embryo: misconceptions and misinterpretations in preimplantation genetic testing for aneuploidy. *Fertil. Steril.* *116*, 1205–1211.

Ven, K. van der, Montag, M., and Ven, H. van der (2008). Polar Body Diagnosis – A Step in The Right Direction? *Dtsch. Arztebl. Int.*

Verpoest, W., Staessen, C., Bossuyt, P.M., Goossens, V., Altarescu, G., Bonduelle, M., Devesa, M., Eldar-Geva, T., Gianaroli, L., Griesinger, G., et al. (2018). Preimplantation genetic testing for aneuploidy by microarray analysis of polar bodies in advanced maternal age: a randomized clinical trial. *Hum. Reprod.* *33*, 1767–1776.

Victor, A.R., Tyndall, J.C., Brake, A.J., Lepkowsky, L.T., Murphy, A.E., Griffin, D.K., McCoy, R.C., Barnes, F.L., Zouves, C.G., and Viotti, M. (2019). One hundred mosaic embryos transferred prospectively in a single clinic: exploring when and why they result in healthy pregnancies. *Fertil. Steril.* *111*, 280–293.

Viotti, M., Victor, A.R., Barnes, F.L., Zouves, C.G., Besser, A.G., Grifo, J.A., Cheng, E.-H., Lee, M.-S., Horcajadas, J.A., Corti, L., et al. (2021). Using outcome data from one thousand mosaic embryo transfers to formulate an embryo ranking system for clinical use. *Fertil. Steril.* *115*, 1212–1224.

Walters-Sen, L., Neitzel, D., Bristow, S.L., Mitchell, A., Alouf, C.A., Aradhya, S., and Faulkner, N. (2021). Experience analyzing >190,000 embryo trophectoderm biopsies using a novel FAST-SeqS PGT assay. *Reprod. Biomed. Online.*

Wei, S., Weiss, Z.R., Gaur, P., Forman, E., and Williams, Z. (2018). Rapid preimplantation genetic screening using a handheld, nanopore-based DNA sequencer. *Fertil. Steril.* *110*, 910-916.e2.

Wei, S., Djandji, A., Lattin, M.T., Nahum, O., Hoffman, N., Cujar, C., Kayali, R., Cinnioglu, C., Wapner, R., D’Alton, M., et al. (2022). Rapid Nanopore Sequencing-Based Screen for Aneuploidy in Reproductive Care. *N. Engl. J. Med.* *387*, 658–660.

Wong, K.M., van Wely, M., Verhoeve, H.R., Kaaijk, E.M., Mol, F., van der Veen, F., Repping, S., and Mastenbroek, S. (2021). Transfer of fresh or frozen embryos: a randomised controlled trial. *Hum. Reprod.* *36*, 998–1006.

Figure and Table Legends:

Figure 1: Study design including concordance rates found in this study. WGA: whole-genome amplification; PGT-A: preimplantation-genetic testing for aneuploidy; aCGH: array comparative-genomic hybridization; PPV and NPV: positive and negative predictive value.

Figure 2: Schematic overview of the nanopore sequencing workflow, including time measures for individual procedures, embedded in the clinical PGT-A workflow. Prorate sequencing time per sample was calculated according to medium sequencing time for 6 pooled samples. Separate sequencing of one sample can be shorter. ICSI: intra-cytoplasmic sperm injection; PB: polar body; WGA: whole-genome amplification.

Figure 3: Occurrence of whole-chromosome aneuploidies in all 99 pooled PB samples. TP: true positive, FN: false negative, FP: false positive.

Figure 4: Example chromosomal distribution plots from automatically generated nanopore sequencing workflow. Quality values noise and MAPD are mapped for each chromosome and thresholds for the total sample (0.6 and 1.7, respectively) are highlighted in red. MAPD: Median of the Absolute values of all Pairwise Differences; noise: median standard deviation of normalised read counts within each segment.

Figure 5: Comparison of nanopore sequencing workflow with and without Endonuclease I digest. EN: Endonuclease I digest.

Table 1: Nanopore sequencing results in comparison with aCGH.

Figure 1:

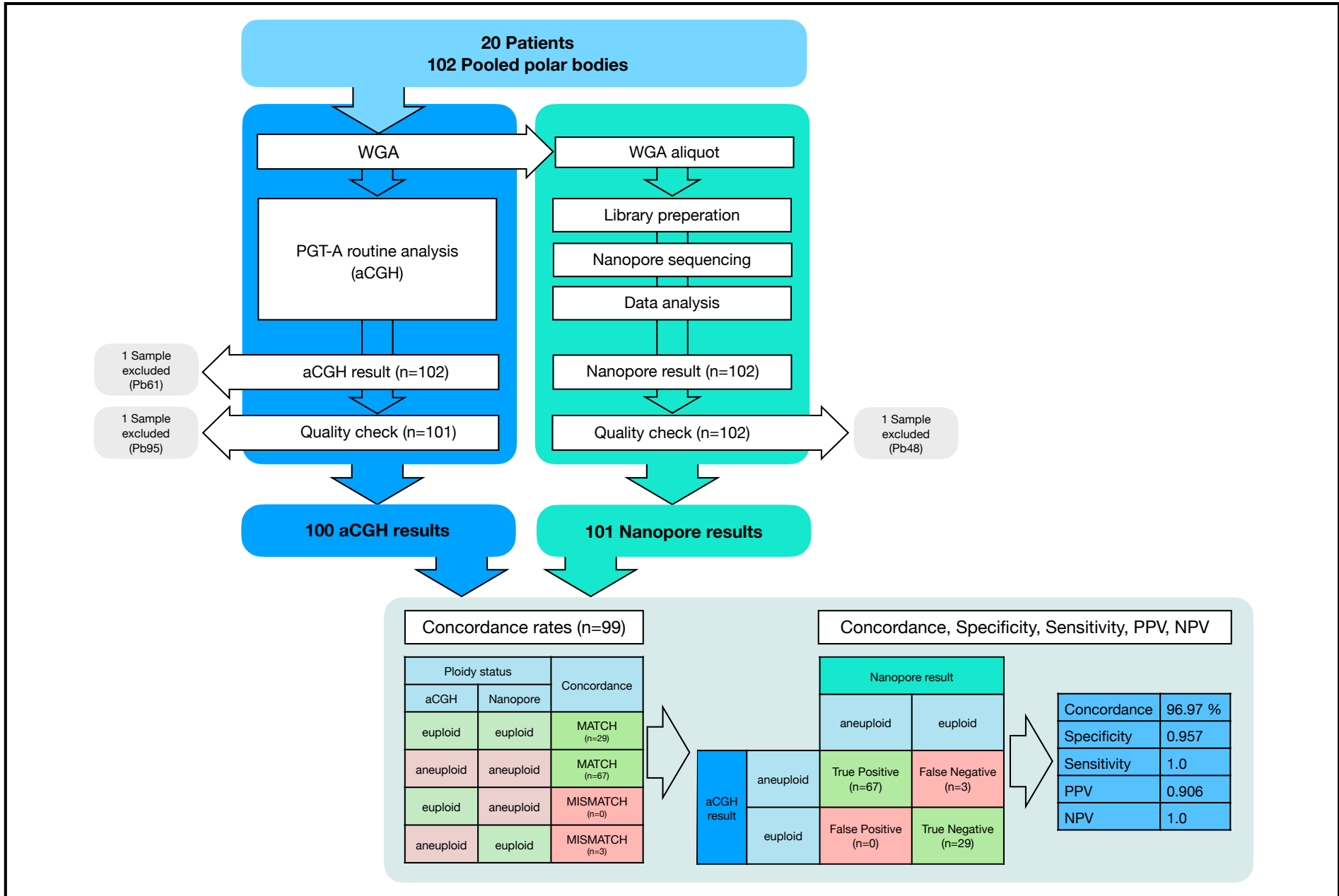


Figure 2:

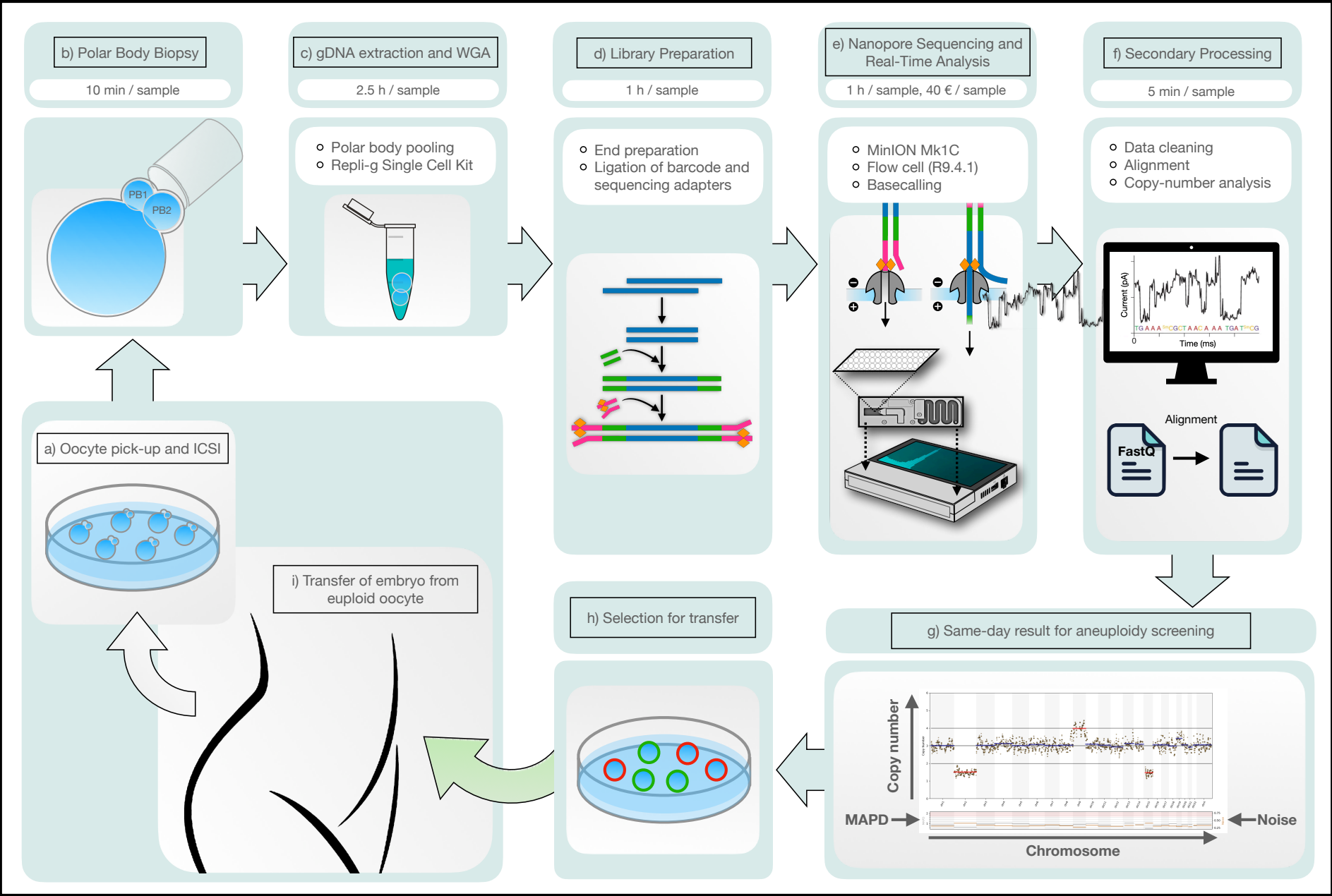
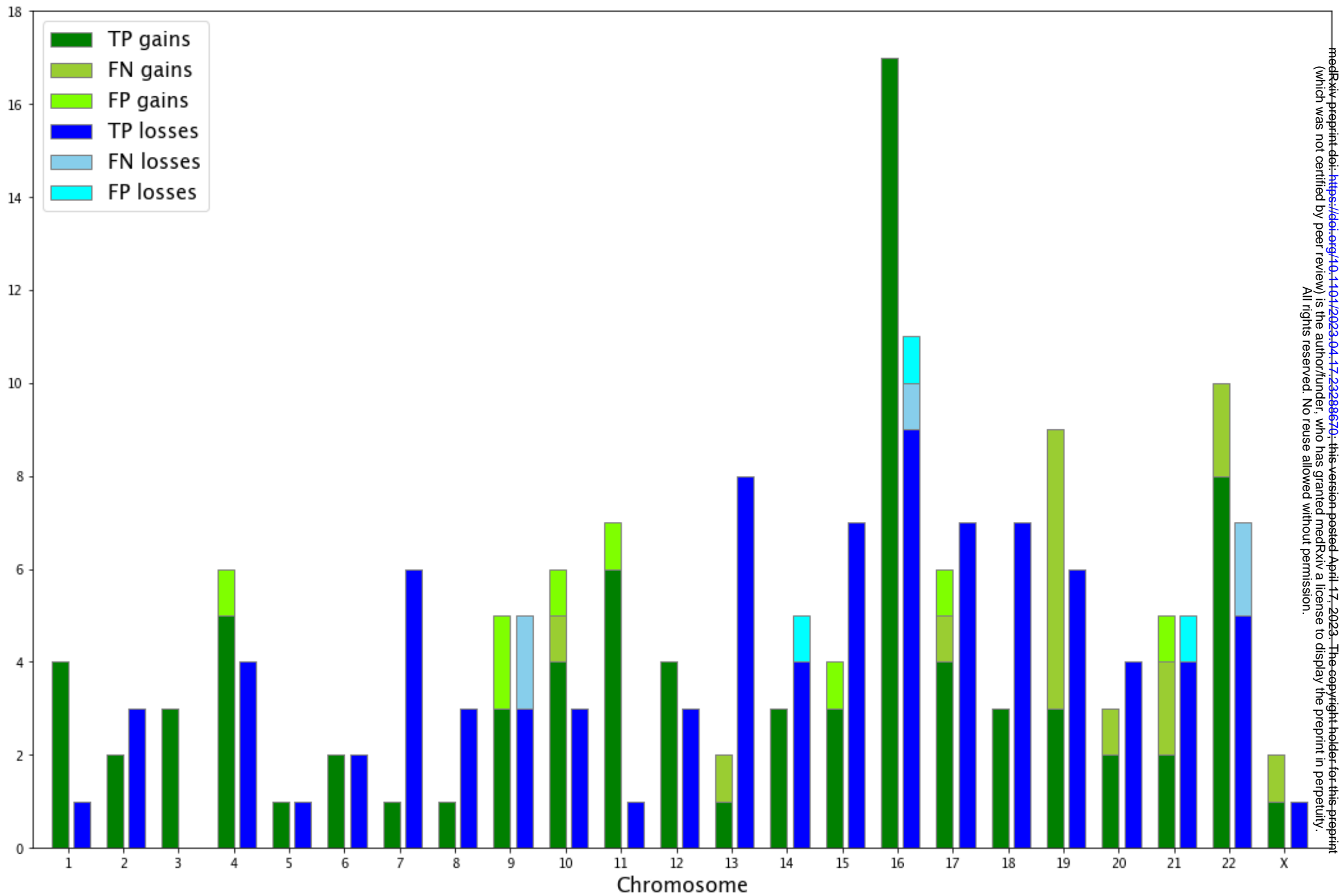


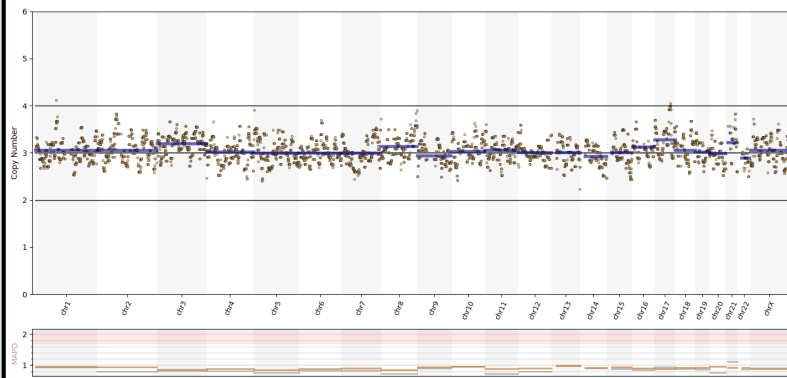
Figure 3:



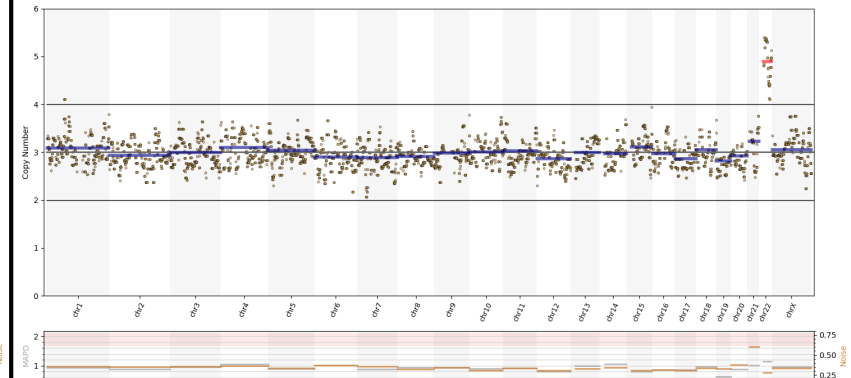
medRxiv preprint doi: <https://doi.org/10.1101/2023.04.17.23288670>; this version posted April 17, 2023. The copyright holder for this preprint (which was not certified by peer review) is the author/funder, who has granted medRxiv a license to display the preprint in perpetuity. All rights reserved. No reuse allowed without permission.

Figure 4:

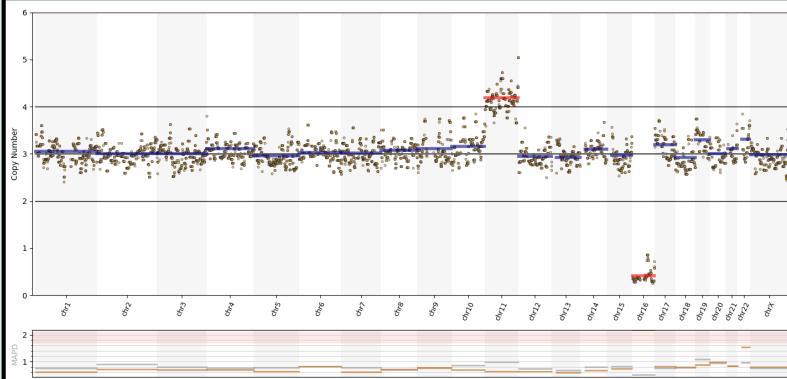
a) euploid



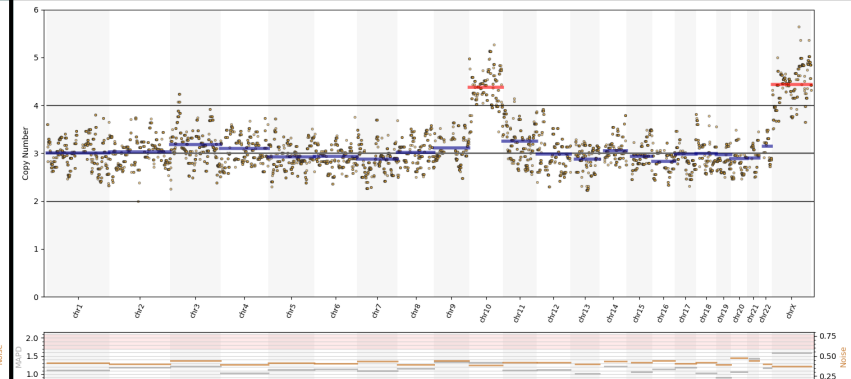
b) aneuploid (+Chr. 22)



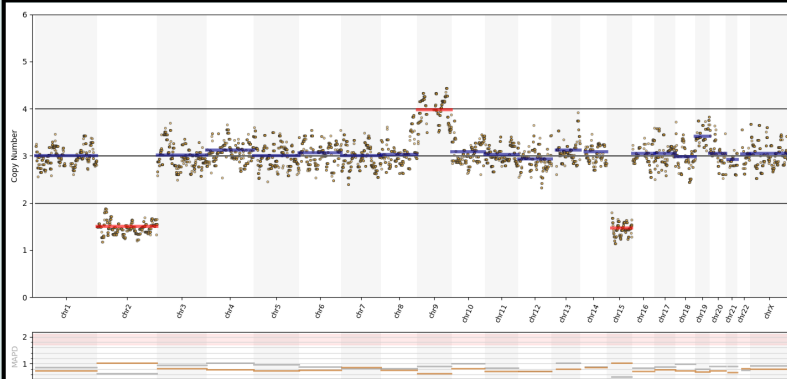
c) aneuploid (+Chr. 11, -Chr. 16)



d) aneuploid (+Chr. 10, +Chr. X)



e) aneuploid (-Chr. 2, +Chr. 9, -Chr. 15)



f) aneuploid (multiple)

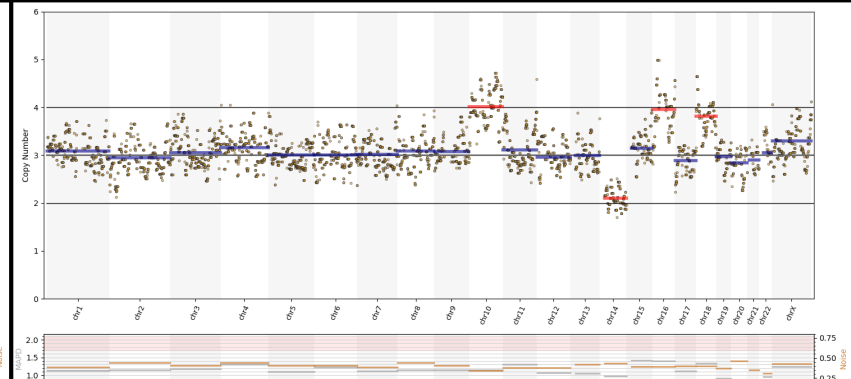
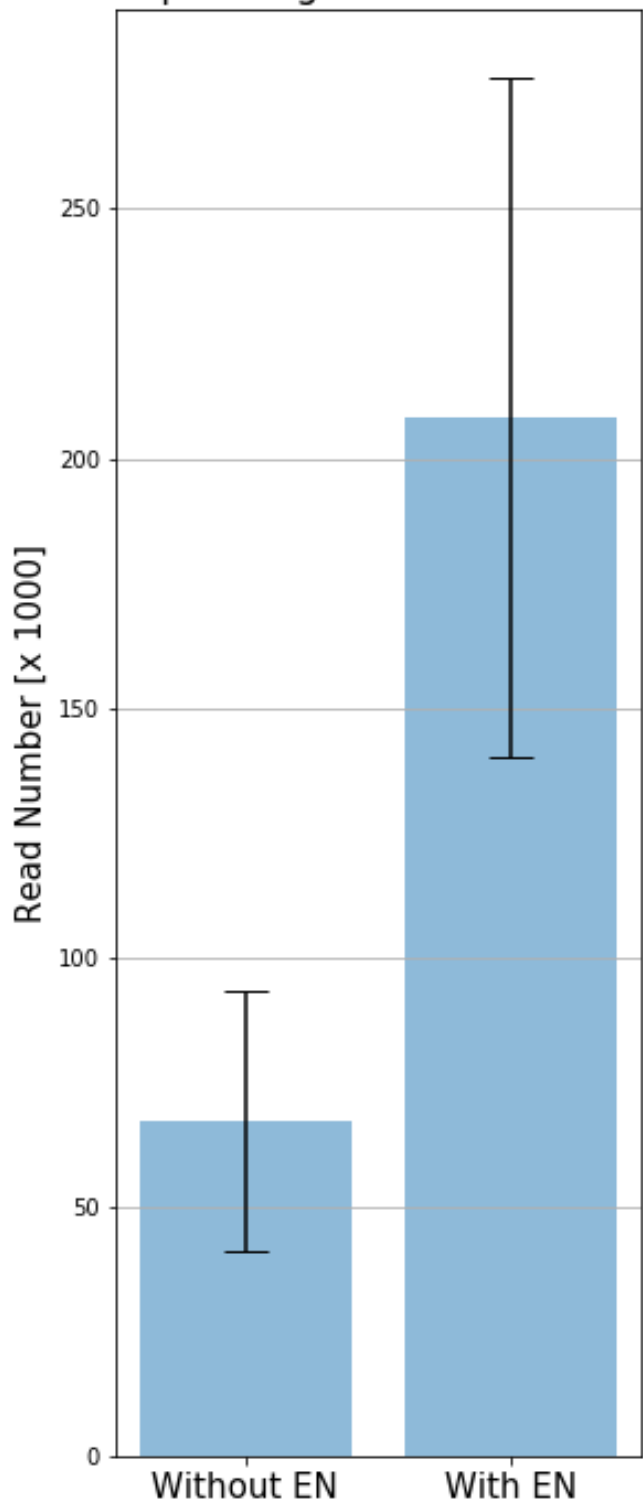
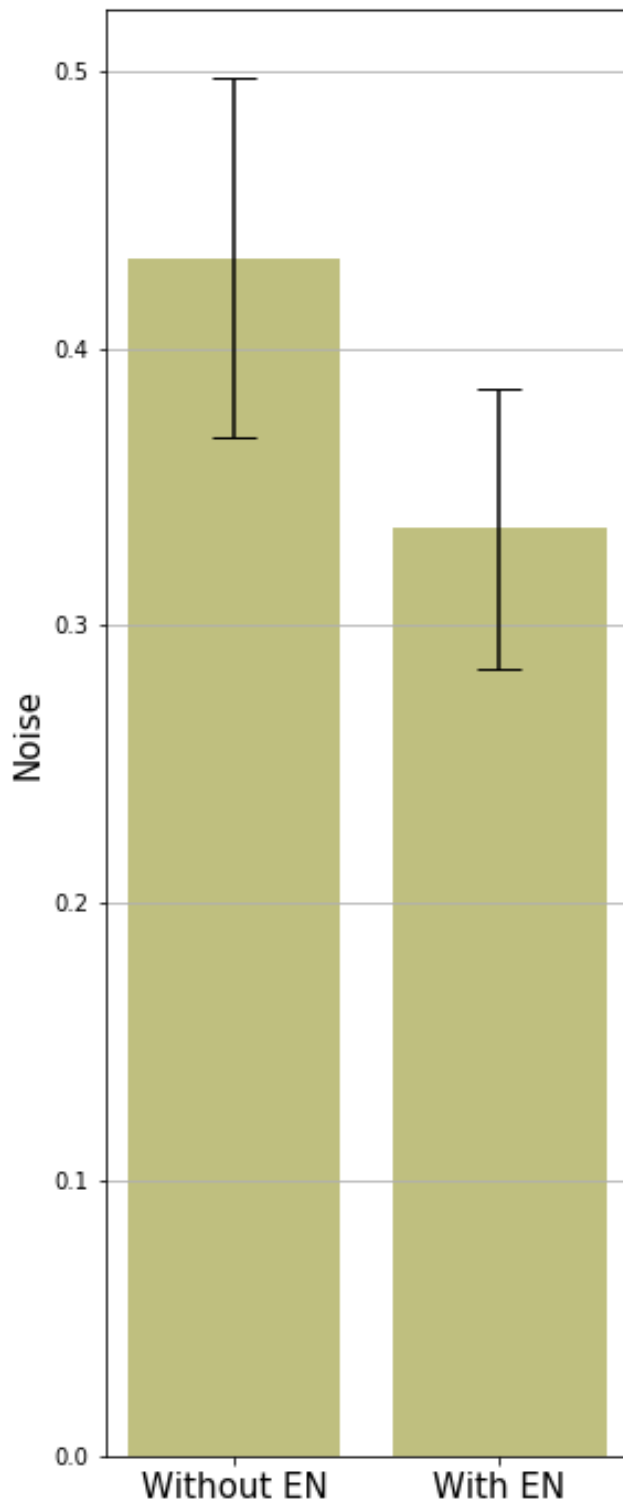


Figure 5: Sequencing Reads Generated



Noise Measured



Full Karyotype Concordance

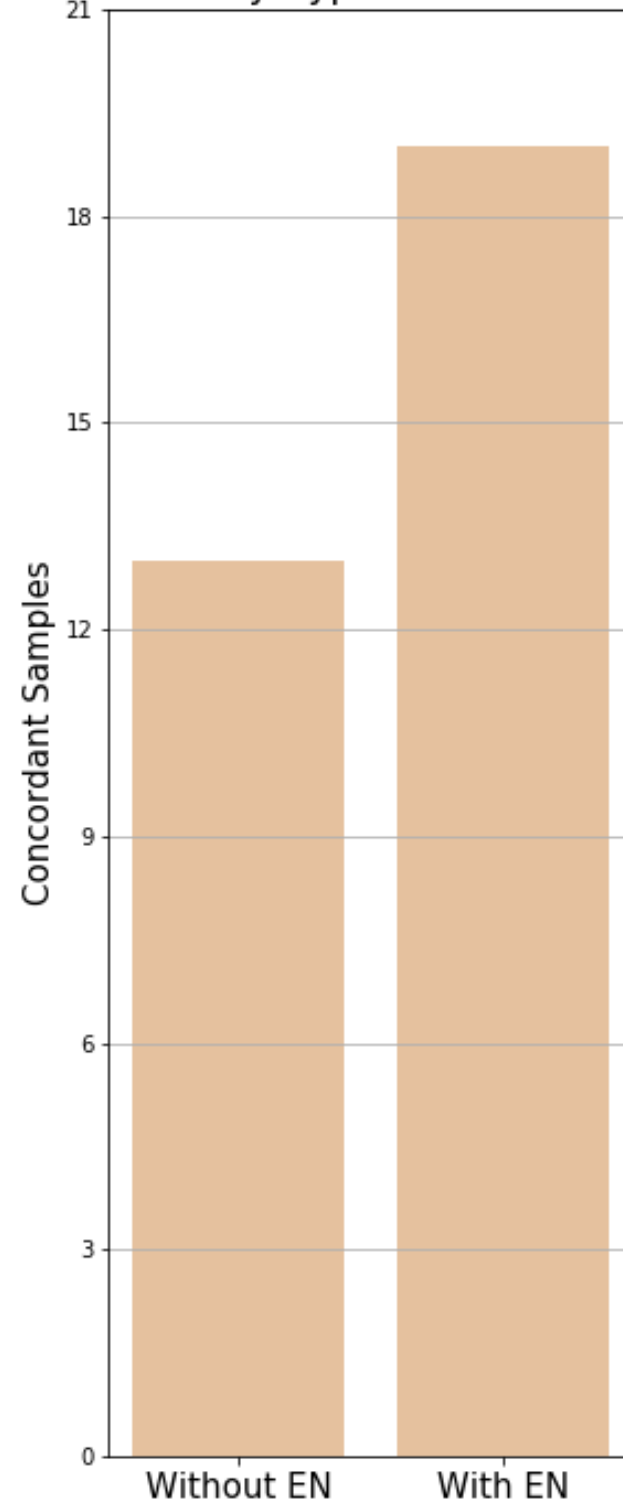


Table 1:

Sample Number	Ploidy Status			Chromosome Aberrations		
	aCGH	Nanopore	Concordance	aCGH	Nanopore	Concordance
Pb1	aneuploid	aneuploid	CONCORDANT	multiple	multiple	CONCORDANT
Pb2	aneuploid	aneuploid	CONCORDANT	+22	+22	CONCORDANT
Pb3	euploid	euploid	CONCORDANT	-	-	CONCORDANT
Pb4	euploid	euploid	CONCORDANT	-	-	CONCORDANT
Pb5	aneuploid	aneuploid	CONCORDANT	-1	-1	CONCORDANT
Pb6	euploid	euploid	CONCORDANT	-	-	CONCORDANT
Pb7	euploid	euploid	CONCORDANT	-	-	CONCORDANT
Pb8	euploid	euploid	CONCORDANT	-	-	CONCORDANT
Pb9	aneuploid	aneuploid	CONCORDANT	multiple	multiple	CONCORDANT
Pb10	euploid	euploid	CONCORDANT	-	-	CONCORDANT
Pb11	aneuploid	aneuploid	CONCORDANT	-4	-4	CONCORDANT
Pb12	euploid	euploid	CONCORDANT	-	-	CONCORDANT
Pb13	aneuploid	aneuploid	CONCORDANT	-15	-15	CONCORDANT
Pb14	euploid	euploid	CONCORDANT	-	-	CONCORDANT
Pb15	aneuploid	aneuploid	CONCORDANT	-10,+14	-10,+14	CONCORDANT
Pb16	aneuploid	aneuploid	CONCORDANT	+10,+X	+10,+X	CONCORDANT
Pb17	aneuploid	aneuploid	CONCORDANT	-14,+20	-14,+20	CONCORDANT
Pb18	aneuploid	aneuploid	CONCORDANT	multiple	multiple	CONCORDANT
Pb19	aneuploid	aneuploid	CONCORDANT	+16,-18,-20	+16,-18,-20	CONCORDANT
Pb20	aneuploid	aneuploid	CONCORDANT	-7,+16	multiple	DISCORDANT
Pb21	aneuploid	aneuploid	CONCORDANT	+19,-21,-22	-21	DISCORDANT
Pb22	aneuploid	aneuploid	CONCORDANT	+12,-13,-16	+12,-13,-16	CONCORDANT
Pb23	euploid	euploid	CONCORDANT	-	-	CONCORDANT
Pb24	euploid	euploid	CONCORDANT	-	-	CONCORDANT
Pb25	euploid	euploid	CONCORDANT	-	-	CONCORDANT
Pb26	aneuploid	aneuploid	CONCORDANT	-16	-16	CONCORDANT
Pb27	euploid	euploid	CONCORDANT	-	-	CONCORDANT
Pb28	aneuploid	aneuploid	CONCORDANT	-6,-12	-6,-12	CONCORDANT
Pb29	euploid	euploid	CONCORDANT	-	-	CONCORDANT
Pb30	aneuploid	aneuploid	CONCORDANT	+11,+15,+22	+11,+15,+22	CONCORDANT
Pb31	aneuploid	aneuploid	CONCORDANT	-17	-17	CONCORDANT
Pb32	aneuploid	aneuploid	CONCORDANT	multiple	multiple	CONCORDANT
Pb33	aneuploid	aneuploid	CONCORDANT	multiple	multiple	CONCORDANT
Pb34	aneuploid	aneuploid	CONCORDANT	-13,-15,-21	-13,-15,-21	CONCORDANT
Pb35	aneuploid	aneuploid	CONCORDANT	-22	-22	CONCORDANT
Pb36	euploid	euploid	CONCORDANT	-	-	CONCORDANT
Pb37	aneuploid	aneuploid	CONCORDANT	+16	+16	CONCORDANT
Pb38	euploid	euploid	CONCORDANT	-	-	CONCORDANT
Pb39	aneuploid	aneuploid	CONCORDANT	multiple	multiple	CONCORDANT
Pb40	aneuploid	aneuploid	CONCORDANT	+4	+4	CONCORDANT
Pb41	aneuploid	aneuploid	CONCORDANT	multiple	multiple	CONCORDANT
Pb42	aneuploid	aneuploid	CONCORDANT	multiple	multiple	CONCORDANT
Pb43	aneuploid	aneuploid	CONCORDANT	multiple	multiple	CONCORDANT
Pb44	aneuploid	aneuploid	CONCORDANT	+15	+15	CONCORDANT
Pb45	aneuploid	aneuploid	CONCORDANT	+16,-19	+16,-19	CONCORDANT
Pb46	aneuploid	euploid	DISCORDANT	+22	-	DISCORDANT
Pb47	aneuploid	aneuploid	CONCORDANT	multiple	multiple	CONCORDANT
Pb48	euploid	not evaluable	EXCLUDED	-	-	EXCLUDED
Pb49	euploid	euploid	CONCORDANT	-	-	CONCORDANT
Pb50	euploid	euploid	CONCORDANT	-	-	CONCORDANT
Pb51	aneuploid	aneuploid	CONCORDANT	multiple	multiple	CONCORDANT
Pb52	euploid	euploid	CONCORDANT	-	-	CONCORDANT
Pb53	euploid	euploid	CONCORDANT	-	-	CONCORDANT
Pb54	aneuploid	aneuploid	CONCORDANT	-9,-15	-9,-15	CONCORDANT
Pb55	aneuploid	aneuploid	CONCORDANT	-17,-18	-17,-18	CONCORDANT
Pb56	aneuploid	aneuploid	CONCORDANT	-16	-16	CONCORDANT
Pb57	euploid	euploid	CONCORDANT	-	-	CONCORDANT
Pb58	aneuploid	aneuploid	CONCORDANT	-13,-14,+17	multiple	DISCORDANT
Pb59	aneuploid	aneuploid	CONCORDANT	multiple	multiple	CONCORDANT
Pb60	euploid	euploid	CONCORDANT	-	-	CONCORDANT
Pb61	not evaluable	euploid	EXCLUDED	-	-	EXCLUDED
Pb62	aneuploid	euploid	DISCORDANT	+19	-	DISCORDANT
Pb63	aneuploid	aneuploid	CONCORDANT	multiple	multiple	CONCORDANT
Pb64	aneuploid	aneuploid	CONCORDANT	+4	+4	CONCORDANT
Pb65	aneuploid	aneuploid	CONCORDANT	+16	+16	CONCORDANT
Pb66	aneuploid	aneuploid	CONCORDANT	multiple	multiple	CONCORDANT
Pb67	aneuploid	aneuploid	CONCORDANT	+12,-15	+12,-15	CONCORDANT
Pb68	aneuploid	aneuploid	CONCORDANT	+2	+2	CONCORDANT
Pb69	aneuploid	aneuploid	CONCORDANT	+6,-18	+6,-18	CONCORDANT
Pb70	aneuploid	aneuploid	CONCORDANT	-16,-22	-16,-22	CONCORDANT
Pb71	aneuploid	aneuploid	CONCORDANT	+11,+16,-17	+11,+16,-17	CONCORDANT
Pb72	aneuploid	aneuploid	CONCORDANT	-19	-19	CONCORDANT
Pb73	aneuploid	aneuploid	CONCORDANT	+4,-20	+4,-20	CONCORDANT
Pb74	aneuploid	aneuploid	CONCORDANT	-16,+21	-16,+21	CONCORDANT
Pb75	aneuploid	aneuploid	CONCORDANT	+16,+22	+16,+22	CONCORDANT
Pb76	euploid	euploid	CONCORDANT	-	-	CONCORDANT
Pb77	euploid	euploid	CONCORDANT	-	-	CONCORDANT
Pb78	aneuploid	aneuploid	CONCORDANT	+17,-22	+17,-22	CONCORDANT
Pb79	aneuploid	aneuploid	CONCORDANT	+18	+18	CONCORDANT
Pb80	euploid	euploid	CONCORDANT	-	-	CONCORDANT
Pb81	euploid	euploid	CONCORDANT	-	-	CONCORDANT
Pb82	aneuploid	aneuploid	CONCORDANT	+9,-13	+9,-13	CONCORDANT
Pb83	aneuploid	aneuploid	CONCORDANT	+16,-19	+16,-19	CONCORDANT
Pb84	aneuploid	aneuploid	CONCORDANT	+1	+1	CONCORDANT
Pb85	aneuploid	euploid	DISCORDANT	-16	-	DISCORDANT
Pb86	aneuploid	aneuploid	CONCORDANT	multiple	multiple	CONCORDANT
Pb87	aneuploid	aneuploid	CONCORDANT	+20	+20	CONCORDANT
Pb88	aneuploid	aneuploid	CONCORDANT	-17	-17	CONCORDANT
Pb89	aneuploid	aneuploid	CONCORDANT	+22	+22	CONCORDANT
Pb90	aneuploid	aneuploid	CONCORDANT	multiple	multiple	CONCORDANT
Pb91	aneuploid	aneuploid	CONCORDANT	-2,+6	-2,+6	CONCORDANT
Pb92	aneuploid	aneuploid	CONCORDANT	multiple	multiple	CONCORDANT
Pb93	aneuploid	aneuploid	CONCORDANT	+1,-16,+19	+1,-16	DISCORDANT
Pb94	euploid	euploid	CONCORDANT	-	-	CONCORDANT
Pb95	not evaluable	euploid	EXCLUDED	-	-	EXCLUDED
Pb96	aneuploid	aneuploid	CONCORDANT	+11,-16,+19	+11,-16	DISCORDANT
Pb97	aneuploid	aneuploid	CONCORDANT	+16	+16	CONCORDANT
Pb98	aneuploid	aneuploid	CONCORDANT	-4	-4	CONCORDANT
Pb99	aneuploid	aneuploid	CONCORDANT	+16	+16	CONCORDANT
Pb100	euploid	euploid	CONCORDANT	-	-	CONCORDANT
Pb101	euploid	euploid	CONCORDANT	-	-	CONCORDANT
Pb102	euploid	euploid	CONCORDANT	-	-	CONCORDANT